International Journal of Nanomedicine

Dovepress
open access to scientific and medical research

Open Access Full Text Article

ORIGINAL RESEARCH

VCAM-1-targeted core/shell nanoparticles for selective adhesion and delivery to endothelial cells with lipopolysaccharide-induced inflammation under shear flow and cellular magnetic resonance imaging in vitro

This article was published in the following Dove Press journal:
International Journal of Nanomedicine
10 May 2013
Number of times this article has been viewed

Hong Yang[1]
Fenglong Zhao[1]
Ying Li[1]
Mingming Xu[1]
Li Li[1]
Chunhui Wu[1]
Hirokazu Miyoshi[2]
Yiyao Liu[1]

[1]Department of Biophysics, School of Life Science and Technology, University of Electronic Science and Technology of China, Chengdu, Sichuan, People's Republic of China; [2]Radioisotope Research Center, University of Tokushima, Kuramoto-cho, Tokushima, Japan

Correspondence: Yiyao Liu
Department of Biophysics,
School of Life Science and Technology,
University of Electronic Science and Technology of China, Chengdu 610054,
Sichuan, People's Republic of China
Tel +86 28 8320 3353
Fax +86 28 8320 8238
Email liuyiyao@hotmail.com

Abstract: Multifunctional nanomaterials with unique magnetic and luminescent properties have broad potential in biological applications. Because of the overexpression of vascular cell adhesion molecule-1 (VCAM-1) receptors in inflammatory endothelial cells as compared with normal endothelial cells, an anti-VCAM-1 monoclonal antibody can be used as a targeting ligand. Herein we describe the development of multifunctional core-shell Fe_3O_4@SiO_2 nanoparticles with the ability to target inflammatory endothelial cells via VCAM-1, magnetism, and fluorescence imaging, with efficient magnetic resonance imaging contrast characteristics. Superparamagnetic iron oxide and fluorescein isothiocyanate (FITC) were loaded successfully inside the nanoparticle core and the silica shell, respectively, creating VCAM-1-targeted Fe_3O_4@SiO_2(FITC) nanoparticles that were characterized by scanning electron microscopy, transmission electron microscopy, fluorescence spectrometry, zeta potential assay, and fluorescence microscopy. The VCAM-1-targeted Fe_3O_4@SiO_2(FITC) nanoparticles typically had a diameter of 355 ± 37 nm, showed superparamagnetic behavior at room temperature, and cumulative and targeted adhesion to an inflammatory subline of human umbilical vein endothelial cells (HUVEC-CS) activated by lipopolysaccharide. Further, our data show that adhesion of VCAM-1-targeted Fe_3O_4@SiO_2(FITC) nanoparticles to inflammatory HUVEC-CS depended on both shear stress and duration of exposure to stress. Analysis of internalization into HUVEC-CS showed that the efficiency of delivery of VCAM-1-targeted Fe_3O_4@SiO_2(FITC) nanoparticles was also significantly greater than that of nontargeted Fe_3O_4@SiO_2(FITC)-NH_2 nanoparticles. Magnetic resonance images showed that the superparamagnetic iron oxide cores of the VCAM-1-targeted Fe_3O_4@SiO_2(FITC) nanoparticles could also act as a contrast agent for magnetic resonance imaging. Taken together, the cumulative adhesion and uptake potential of these VCAM-1-targeted Fe_3O_4@SiO_2(FITC) nanoparticles targeted to inflammatory endothelial cells could be used in the transfer of therapeutic drugs/genes into these cells or for diagnosis of vascular disease at the molecular and cellular levels in the future.

Keywords: silica nanoparticles, vascular cell adhesion molecule-1, endothelial cells, adhesion, magnetic resonance imaging

Introduction

In recent years, there has been increasing interest in fabricating carriers in the nanometer and micrometer range with important applications in biomedicine. Of these, magnetic nanoparticles, eg, Fe_3O_4, are a promising candidate because of their wide range of sophisticated biomedical applications, including targeted drug delivery, magnetic hyperthermia, magnetic resonance imaging, biosensing, and magnetic separation of biological materials.[1–3] Although magnetic nanoparticles have many advantages as magnetic carriers, they have at least two limitations. One is poor dispersion with easy aggregation and the other is the limited number of functional groups on their surfaces. To overcome these limitations, modifications have been made by adding surface coatings to the magnetic nanoparticles. In addition to its well developed surface chemistry, silica is considered to be an exceptional material for encapsulating magnetic nanoparticles because of its good biocompatibility, excellent physicochemical stability, and ease of multifunctionalization.[2,4]

In general, coating of Fe_3O_4 nanoparticles with silica can be achieved using the Stöber process and the reverse (water-in-oil) microemulsion method.[5,6] Using the reverse microemulsion method, it has been shown that aqueous Fe_3O_4 nanoparticles can be incorporated within silica to form core/shell silica particles with single Fe_3O_4 cores[7] which can efficiently label human mesenchymal stem cells. However, the superparamagnetic behavior and saturation of magnetization decreases after coating with silica. One possible strategy is to encapsulate more Fe_3O_4 cores into the silica shell,[8] which would create hybrid silica nanoparticles with a large magnetic component. Consequently, the superparamagnetic behavior, saturation of magnetization, and magnetic resonance signal intensity is significantly increased. Other studies have shown that the magnetic core can be replaced by semiconductor quantum dots or fluorescence molecules doped into the silica shell to form fluorescent core/shell silica nanoparticles.[9–11] These silica-coated fluorescent magnetic nanoprobes enabled development of biomedical platforms for simultaneous imaging, diagnosis, and therapy.[12–14] However, it is still a challenge to fabricate fluorescent magnetic nanoprobes with high photostability, high payloads of dye, and desirable outer surfaces for further modification with functional or target moieties.

Avoiding nonspecific delivery is another important concern in the design of nanoparticles. An attractive means of targeted delivery is use of cell-specific targeting ligands linked to nanoparticle surfaces, because these enhance adhesion and cellular uptake (internalization) of nanoparticles via use of unique molecular markers that are preferentially overexpressed in diseased tissue. This strategy is particularly effective for receptor-mediated endocytosis using specific ligands to recognize their receptors on cell membranes.

Inflammation and endothelial dysfunction are major threshold developments in the progression of atherosclerosis. Expression of endothelial cell adhesion molecules, eg, vascular cell adhesion molecule-1 (VCAM-1), plays an important role in recruitment of leukocytes, and is often increased at sites of pathological inflammation. Persistent expression of VCAM-1 in dysfunctional endothelial cells mediates adhesion, rolling, and tethering of mononuclear leukocytes and facilitates their transmigration to developing atherosclerotic plaques. Previous studies, including those of our group, have reported overexpression of VCAM-1 and/or other cell adhesion molecules associated with endothelial cell dysfunction and progression of atherosclerosis.[15,16] Therefore, VCAM-1 is a potential marker and ideal target for drug/gene delivery and early detection by imaging.

Herein we report a new class of multifunctional VCAM-1-targeted Fe_3O_4@SiO_2(FITC) nanoparticles. We used a parallel flow chamber system to investigate adhesion of these nanoparticles on a monolayer of endothelial cells under controlled shear conditions. Using confocal laser microscope and flow cytometry, we confirmed that the VCAM-1-targeted Fe_3O_4@SiO_2(FITC) nanoparticles accumulated on the surfaces of endothelial cells with high efficiency. Moreover, we demonstrated that these biofunctionalized nanoparticles could be used as both fluorescent and magnetic imaging probes at the cellular level. These nanoparticles are expected to be an important candidate for enhancing contrast in diagnostic imaging for atherosclerosis in the future.

Materials and methods

Chemicals and materials

Polyoxyethylene(5) nonylphenylether (Igepal CO-520), tetraethylorthosilicate, 3-aminopropyltrimethoxysilane (APS), fluorescein isothiocyanate (FITC), N-(3-dimethylaminopropyl)-N′-ethylcarbodiimide hydrochloride, N-hydroxysuccinimide, sodium silicate solution ($Na_2O(SiO_2)_{3-5}$, 27 wt% SiO_2), and lipopolysaccharide were obtained from Sigma-Aldrich (St Louis, MO, USA). Iron oxide nanoparticles (10 nm) were obtained from Nanjing Emperor Nano Material Co, Ltd (Nanjing, People's Republic of China). RPMI-1640 cell culture medium, newborn calf serum, and trypsin were purchased from Gibco (Grand Island, NY, USA). A phycoerythrin-labeled anti-VCAM-1 monoclonal antibody was obtained from BioLegend (San Diego, CA, USA). All chemicals were used as received without further purification.

Synthesis of VCAM-1-targeted Fe_3O_4@SiO_2(FITC) nanoparticles

Fe_3O_4@SiO_2(FITC) nanoparticles were synthesized by hydrolysis and condensation of tetraethylorthosilicate in an ammonia ethanol/water solution in the presence of iron oxide particles and FITC using a modification of a previously reported sol-gel method.[10,17,18] Briefly, 2 mg of FITC was reacted with 125 μL of APS in 1 mL of anhydrous ethanol in the dark at room temperature for 24 hours. The reaction solution of FITC-APS conjugates was then stored at 4°C. Next, 1 mL of aqueous solution containing magnetic particles was diluted with 1 mL of water and 7.5 mL of anhydrous ethanol; 300 μL of tetraethylorthosilicate and ammonia solution (28–30 wt% by NH_3) were added to this reaction mixture while stirring at 300 rpm for 24 hours at room temperature, followed by addition of an as-synthesized APS-FITC solution with continuous stirring for 48 hours. The reaction was terminated by adding methanol. The Fe_3O_4@SiO_2(FITC) particles were separated and washed several times with Milli-Q water (Millipore, Billerica, MA, USA).

The Fe_3O_4@SiO_2(FITC) nanoparticles obtained were resuspended in 5 mL of anhydrous acetic acid (1 mM), and reacted further with 200 μL of APS in a sealed vessel. The reaction was allowed to proceed at room temperature for 24 hours with gentle stirring at 300 rpm. The Fe_3O_4@SiO_2(FITC)-NH_2 nanoparticles were then separated by centrifugation at 12,000 rpm for five minutes and washed five times with deionized water to remove excess reactants.

To attach anti-VCAM-1 monoclonal antibodies to the surfaces of the Fe_3O_4@SiO_2(FITC)-NH_2 nanoparticles, 20 μL of anti-VCAM-1 monoclonal antibody were mixed with 20 mL of N-(3-dimethylaminopropyl)-N′-ethylcarbodiimide hydrochloride and 10 mL of N-hydroxysuccinimide solution, with gentle shaking at 130 rpm for 30 minutes in ice-cold water. The mixture was then added to a flask containing 1 mL of the Fe_3O_4@SiO_2(FITC)-NH_2 nanoparticle suspension and stirred at 300 rpm for 12 hours at room temperature. The VCAM-1-targeted Fe_3O_4@SiO_2(FITC) nanoparticles were then centrifuged and washed with deionized water, finally dispersed in phosphate-buffered saline at 4ºC, and then stored. The procedure used for synthesis of the VCAM-1-targeted Fe_3O_4@SiO_2(FITC) nanoparticles is shown in Figure 1.

Characterization

Particle morphology and size were investigated by scanning electron microscopy (JSM-6490 LV, JEOL, Tokyo, Japan) and transmission electron microscopy (JEM-100CX, JEOL). The size distribution and surface charge on the nanoparticles were

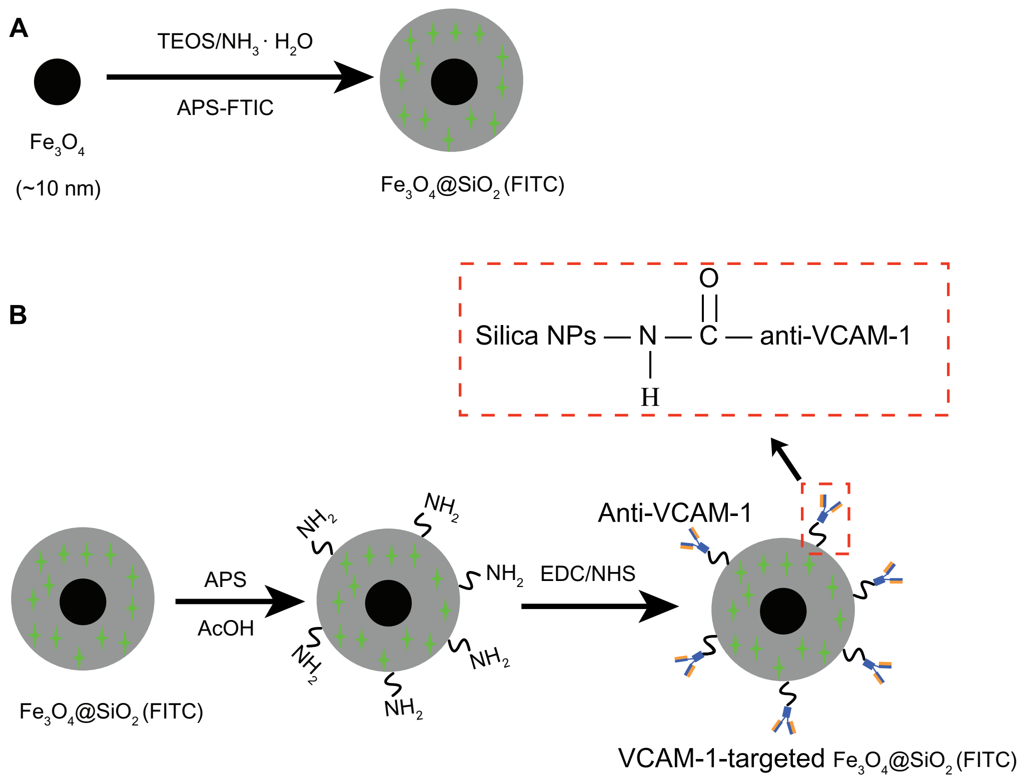

Figure 1 Schematic illustration of the synthesis procedure for VCAM-1-targeted Fe_3O_4@SiO_2(FITC) nanoparticles. (**A**) Fe_3O_4@SiO_2(FITC) nanoparticles were synthesized by reverse microemulsion. (**B**) The coupling agent APS was used to continue the reaction to form Fe_3O_4@SiO_2(FITC)-NH_2 in acetic acid; surface modification of the phycoerythrin-labeled anti-VCAM-1 monoclonal antibody resulted in VCAM-1-targeted Fe_3O_4@SiO_2(FITC) nanoparticles.

Abbreviations: Fe_3O_4@SiO_2(FITC), fluorescein isothiocyanate-loaded silica-coated superparamagnetic iron oxide nanoparticles; VCAM-1, vascular cell adhesion molecule-1; TEOS, tetraethylorthosilicate; NPs, nanoparticles; EDC, N-(3-dimethylaminopropyl)-N′-ethylcarbodiimide; NHS, N-hydroxysuccinimide.

analyzed using a Mastersizer 2000 (Malvern Instruments, Worcestershire, UK) in accordance with the manufacturer's operating manual. The presence of FITC doped into the silica shell was confirmed using an inverted fluorescence microscope (TE-2000U, Nikon, Tokyo, Japan). Magnetic measurement of the samples was performed on a superconducting quantum interference magnetometer (MPMS5S, Quantum Design Inc, San Diego, CA, USA). For measurement, about 10 mg of powder samples was inserted into a gelatin capsule. The magnetic hysteresis loop was measured at room temperature (300 K).

Cell culture

An inflammatory subline of human umbilical vein endothelial cells (HUVEC-CS) was obtained from the American Type Culture Collection (Manassas, VA, USA) and cultured in RPMI-1640 cell culture medium supplemented with 10% newborn calf serum and 1% penicillin-streptomycin.[15] The cells were maintained in an incubator at 37°C with 95% humidity and 5% CO_2, subcultured after trypsinization (0.025% trypsin, 0.5 mM EDTA, 1 mM sodium pyruvate, 10 mM HEPES), and grown to approximately 90% confluence. The HUVEC-CS were then subcultured in 12-well plates at a density of 4×10^4/mL, and maintained in an incubator overnight. The cultured HUVEC-CS were stimulated with 1 μg/mL lipopolysaccharide for five hours to induce inflammation.[19]

Shear flow simulation and nanoparticle adhesion

The interaction (adhesion) between VCAM-1-targeted Fe_3O_4@SiO_2(FITC) nanoparticles and a monolayer of HUVEC-CS was measured in a parallel plate flow chamber at shear stresses of 1.1, 5.15, and 9.94 dynes/cm^2, as previously described by our laboratory.[15,20] In brief, a flow channel in the chamber was constructed using a silicon gasket. The cell-seeded glass slide and the gasket were fastened between a polycarbonate base plate and a stainless plate. The chamber was connected to a perfusion loop system, kept in a constantly temperature-controlled enclosure, and maintained at pH 7.4 by continuous gassing with a humidified mixture of 5% CO_2 in air. Flow of perfusate in a flow channel is laminar with a parabolic velocity profile. The fluid shear stress (τ) generated on the cells seeded on the glass slide can be estimated as $\tau = 6\mu Q/wh^2$, where Q is the flow rate, μ is the dynamic viscosity of the perfusate, w is the width of the flow field, and h is the height.[21] The shear stress can be regulated through the flow rate, Q. Before perfusion, the VCAM-1-targeted Fe_3O_4@SiO_2(FITC) nanoparticle suspension was mixed with the perfusion medium. Adhesion was recorded using an inverted fluorescence microscope. Six random fields (objective magnification 10×) were chosen to quantify the fluorescence intensity on the endothelial cell monolayer.

Specific accumulation on cell surfaces and confocal microscopy

The HUVEC-CS (0.5×10^5 cells/mL) were cultured on coverslips, which were kept in a six-well plate for 12 hours before treatment. After treatment with Fe_3O_4@SiO_2(FITC)-NH_2 or VCAM-1-targeted Fe_3O_4@SiO_2(FITC) nanoparticles with or without lipopolysaccharide stimulation, the cells were washed three times with phosphate-buffered saline (pH 7.4), and then fixed with 4% paraformaldehyde solution in phosphate-buffered saline for 15 minutes at 37°C. The coverslips were then washed three times with phosphate-buffered saline to remove nonspecific binding. Finally, the samples were examined under a confocal laser scanning microscope (FluoView™ FV1000, Olympus, Japan).

Flow cytometry assay

To quantify specific accumulation of the nanoparticles, HUVEC-CS were seeded in 12-well plates at a density of 0.5×10^5 cells/well and allowed to grow for 12 hours. The cells were then activated with lipopolysaccharide 1 μg/mL for five hours. The cells were washed three times with sterilized phosphate-buffered saline, and 2 mL of RPMI-1640 culture medium was then added. The HUVEC-CS were exposed to nanoparticles at a concentration of 850 μg/mL for 12 hours, then washed repeatedly with sterilized phosphate-buffered saline three times, trypsinized, and suspended in phosphate-buffered saline for flow cytometry analysis (FACSCanto II, Becton Dickinson, Franklin Lakes, NJ, USA).

Magnetic resonance imaging in vitro

HUVEC-CS were seeded onto 12-well plates at a density of 0.5×10^5 cells/mL, grown overnight, and then activated with lipopolysaccharide 1 μg/mL for five hours. The cells were washed three times with sterilized phosphate-buffered saline, and 2 mL of RPMI-1640 was then added for 10 hours of culture in the incubator. Next, VCAM-1-targeted Fe_3O_4@SiO_2(FITC) nanoparticles at various concentrations (0, 100, 200, 300, and 400 μg/mL) were added, and a saline solution without any nanoparticles was used as the control. After 12 hours of incubation, the cells were washed three times in phosphate-buffered saline to remove the free nanoparticles, collected, and suspended in 1.5 mL of phosphate-buffered saline containing 1% agarose. Magnetic resonance imaging experiments were performed in a clinical 3.0 Tesla Clinical Siemens Trio scanner (Discovery MR750, GE Healthcare, Boulder, CO, USA). T_2-weighted images were acquired using spin-echo imaging sequences.

Statistical analysis

The quantitative data are presented here as the mean ± standard deviation. Statistical analyses between different groups were performed using one-way analysis of variance followed by Bonferroni tests, and a P value of <0.05 was considered to be statistically significant.

Results and discussion

Magnetic nanoparticles have been attracting interest as a result of their unique properties and potential applications in biomedicine and bioengineering. However, most of these applications require magnetic nanoparticles to be embedded in a nonmagnetic matrix to avoid aggregation and sedimentation, as well as to endow them with particular surface properties for specific applications. This has been attempted by several groups.[22–25] Although few research groups have concentrated on how nanoparticles adhere to targeted cell surfaces, attempts have been directed towards to interactions between targeted nanoparticles and endothelial cells under hemodynamic shear flow conditions.[15,26]

In this study, synthesis of Fe_3O_4@SiO_2(FITC)-NH_2 nanoparticles was based on sol-gel growth of silica in a limited domain of water in water-in-oil microemulsion.[5,27] Using this method, it is possible to grow an iron oxide in a silica core/shell structure of high uniformity (Figure 2). This synthesis process enables coencapsulation of Fe_3O_4 nanoparticles and a large number of FITC dye molecules together within a silica shell. The diameter of the Fe_3O_4@SiO_2(FITC)-NH_2 nanoparticles increased from 331 ± 49 nm (Figure 2A) to 355 ± 37 nm after modification with anti-VCAM-1 monoclonal antibody (Figure 2B). Surface modification of Fe_3O_4@SiO_2(FITC)-NH_2 nanoparticles with phycoerythrin-labeled anti-VCAM-1 monoclonal antibody was likely responsible for the slight increase in particle size. Moreover, these as-synthesized nanoparticles are uniform, and can be well dispersed in aqueous solution, thus making it feasible to measure relaxivity and to run cell experiments. In our earlier report, we also showed that Fe_3O_4@SiO_2(FITC)-NH_2 nanoparticles have low cytotoxicity.[18]

FITC-APS conjugates were prepared in advance via an addition reaction between the isothiocyanate group of FITC dye and the primary amine group of APS. This synthetic process enables the coencapsulation of Fe_3O_4 nanoparticles and a large number of FITC dye molecules together within the silica shell, and grafting of primary amines into the silica surface.[28,29] Using fluorescence microscopy, we confirmed that both Fe_3O_4@SiO_2(FITC)-NH_2 and VCAM-1-targeted Fe_3O_4@SiO_2(FITC) nanoparticles showed well dispersed and distinct fluorescence (Figure 3). We also found that anti-VCAM-1 monoclonal antibody modification had no obvious influence on fluorescence intensity (Figure 3C). The final surface layer incorporating primary amines was formed in situ by hydrolysis of APS. It was confirmed that the zeta potential changed from negative (−20.1 ± 4.1 mV) to positive (8.4 ± 2.9 mV, Figure 4). The zeta potential also did not change significantly, even after modification with anti-VCAM-1 monoclonal antibody. Further, fluorescence spectroscopy was carried out to determine whether anti-VCAM-1 monoclonal antibody molecules conjugated with the Fe_3O_4@SiO_2(FITC)-NH_2 nanoparticle surfaces. The fluorescence emission spectra showed an emission peak at a wavelength of approximately 575 nm for the VCAM-1-targeted Fe_3O_4@SiO_2(FITC) nanoparticle suspension (Figure 5), which is the characteristic

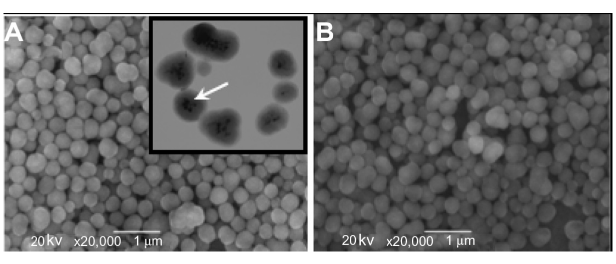

Figure 2 Scanning electron microscopic images of Fe_3O_4@SiO_2(FITC)-NH_2 nanoparticles with a diameter of 331 ± 49 nm (**A**) and VCAM-1-targeted Fe_3O_4@SiO_2(FITC) nanoparticles with a diameter of 355 ± 37 nm (**B**).
Notes: Inset shows a higher magnification transmission electron microscopic image indicating the core/shell structure of Fe_3O_4@SiO_2(FITC)-NH_2 nanoparticles. The Fe_3O_4 nanoparticle core is marked by arrows.
Abbreviations: Fe_3O_4@SiO_2(FITC), fluorescein isothiocyanate-loaded silica-coated superparamagnetic iron oxide nanoparticles; VCAM-1, vascular cell adhesion molecule-1.

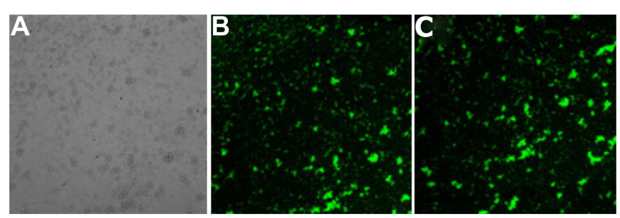

Figure 3 (**A**) Light microscopic images for aqueous suspension of Fe_3O_4@SiO_2(FITC)-NH_2 nanoparticles in solution. (**B** and **C**) Fluorescence microscopy images of aqueous suspension of Fe_3O_4@SiO_2(FITC)-NH_2 and VCAM-1-targeted Fe_3O_4@SiO_2(FITC) nanoparticles in solution, respectively.
Abbreviations: Fe_3O_4@SiO_2(FITC), fluorescein isothiocyanate-loaded silica-coated superparamagnetic iron oxide nanoparticles; VCAM-1, vascular cell adhesion molecule-1.

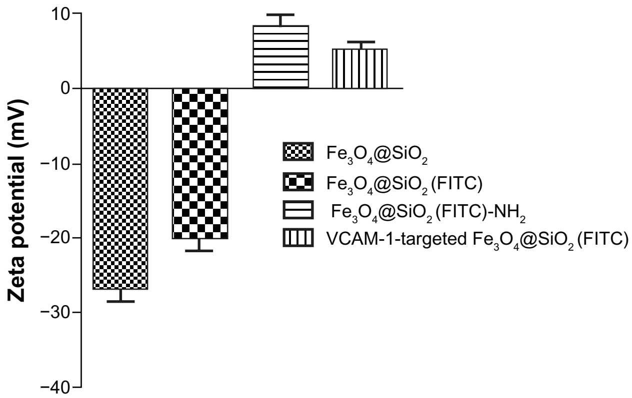

Figure 4 Zeta potential measurements of Fe_3O_4@SiO_2, Fe_3O_4@SiO_2(FITC), Fe_3O_4@SiO_2(FITC)-NH_2 and VCAM-1-targeted Fe_3O_4@SiO_2(FITC) nanoparticles in aqueous suspension.

Abbreviations: Fe_3O_4@SiO_2(FITC), fluorescein isothiocyanate-loaded silica-coated superparamagnetic iron oxide nanoparticles; VCAM-1, vascular cell adhesion molecule-1.

fluorescence emission peak of phycoerythrin.[30] This suggests that anti-VCAM-1 monoclonal antibody molecules were successfully conjugated with the Fe_3O_4@SiO_2(FITC)-NH_2 nanoparticle surfaces. For assessment of the magnetic properties and sensitivity of the formulated Fe_3O_4@SiO_2(FITC)-NH_2 and VCAM-1-targeted Fe_3O_4@SiO_2(FITC), magnetic hysteresis loops were recorded using a magnetometer, and both types of nanoparticles showed superparamagnetic behavior without magnetic hysteresis (Figure 6) at room temperature (about 300 K). They were found to have no coercive fields, thereby confirming their superparamagnetic nature. Their saturation of magnetization was relative low at 3.0 T because

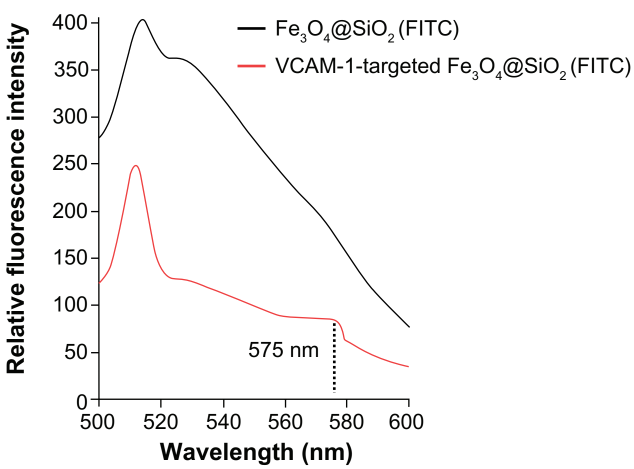

Figure 5 Fluorescence emission spectra of Fe_3O_4@SiO_2(FITC)-NH_2 and VCAM-1-targeted Fe_3O_4@SiO_2(FITC) nanoparticles.

Notes: The fluorescence excitation peak at a wavelength of approximately 575 nm indicates successful coupling of the phycoerythrin-labeled anti-VCAM-1 monoclonal antibody to the particle surfaces.

Abbreviations: Fe_3O_4@SiO_2(FITC), fluorescein isothiocyanate-loaded silica-coated superparamagnetic iron oxide nanoparticles; VCAM-1, vascular cell adhesion molecule-1.

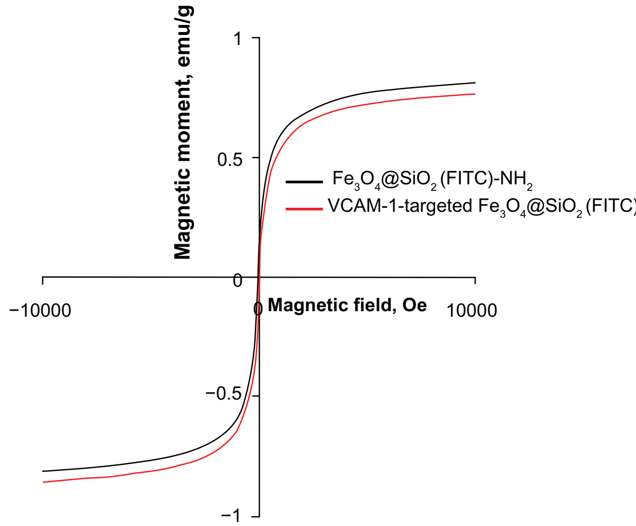

Figure 6 Magnetization curves of Fe_3O_4@SiO_2(FITC)-NH_2 and VCAM-1-targeted Fe_3O_4@SiO_2(FITC) nanoparticles as a function of the applied magnetic field at room temperature (300 K).

Abbreviations: Fe_3O_4@SiO_2(FITC), fluorescein isothiocyanate-loaded silica-coated superparamagnetic iron oxide nanoparticles; VCAM-1, vascular cell adhesion molecule-1.

of the presence of the thick outer silica shell. It is interesting that there was no significant difference in their magnetic hysteresis loops and magnetization saturation values even when the Fe_3O_4@SiO_2(FITC)-NH_2 nanoparticles were modified with the anti-VCAM-1 monoclonal antibody.

The vascular endothelium is a potential target for therapeutic intervention in diverse pathological processes, including inflammation, atherosclerosis, and thrombosis. When targeted nanoparticles enter the bloodstream after injection, they will inevitably interact with endothelial cells, and be retained in the inflamed endothelium via specific endothelial cell adhesion molecules (eg, VCAM-1), expression of which is upregulated on endothelial cell surfaces. This interaction provides the basis for targeted drug/gene delivery or imaging of the abovementioned diseases. Therefore, it was necessary to profile VCAM-1-targeted Fe_3O_4@SiO_2(FITC) adhesion under flow conditions in vitro. Firstly, we compared adhesion with HUVEC-CS between the Fe_3O_4@SiO_2(FITC)-NH_2 and VCAM-1-targeted Fe_3O_4@SiO_2(FITC) nanoparticles under static conditions. We found no significant difference for nontargeted Fe_3O_4@SiO_2(FITC)-NH_2 nanoparticles regardless of activation by lipopolysaccharide (Figure 7). However, the degree of adhesion between VCAM-1-targeted Fe_3O_4@SiO_2(FITC) nanoparticles and HUVEC-CS was markedly higher when the cells were activated by lipopolysaccharide or under a magnetic field, and the degree of adhesion decreased after blocking of the VCAM-1 receptors on the HUVEC-CS surfaces by the anti-VCAM-1 monoclonal

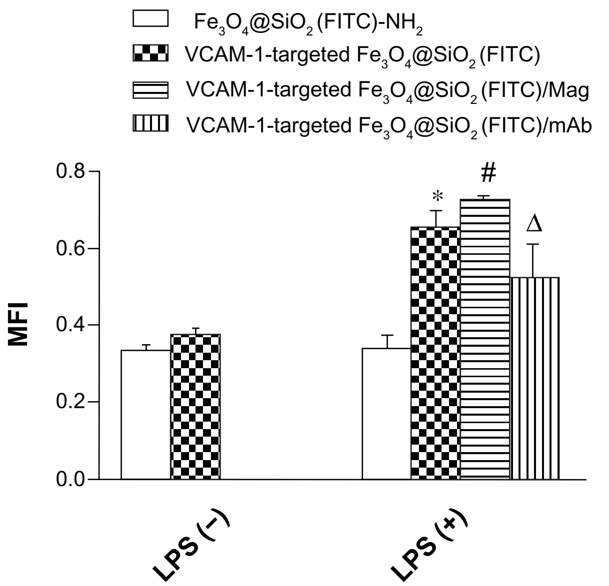

Figure 7 Adhesion of fluorescent nanoparticles on a monolayer of HUVEC-CS under static conditions calculated quantitatively using MFI.

Notes: The nanoparticles were cocultured with HUVEC-CS for 45 minutes, and washed three times with phosphate-buffered saline to remove the nonadhered nanoparticles. The adhered nanoparticles were observed under an inverted fluorescence microscope. *$P < 0.05$ versus $Fe_3O_4@SiO_2$(FITC)-NH_2 at LPS (+); #$P < 0.05$ versus VCAM-1-targeted $Fe_3O_4@SiO_2$(FITC) at LPS (+); Δ$P < 0.05$ versus VCAM-1-targeted $Fe_3O_4@SiO_2$(FITC) at LPS (+) lipopolysaccharide.

Abbreviations: $Fe_3O_4@SiO_2$(FITC), fluorescein isothiocyanate-loaded silica-coated superparamagnetic iron oxide nanoparticles; VCAM-1, vascular cell adhesion molecule-1; MFI, mean fluorescence intensity; LPS, lipopolysaccharide; mAb, monoclonal antibody; LPS (–): no LPS stimulation; LPS (+): stimulation with 1 μg/mL LPS for 5 hours; LPS (+)/Mag: LPS stimulation for 5 hours plus magnetic field; LPS (+)/monoclonal antibody: LPS stimulation for 5 hours plus anti-VCAM-1 monoclonal antibody pretreatment; HUVEC-CS, an inflammatory subline of human umbilical vein endothelial cells.

antibody (Figure 7). It was shown that VCAM-1-targeted $Fe_3O_4@SiO_2$(FITC) nanoparticles could adhere cumulatively and aggregate onto the inflammatory HUVEC-CS, and have the potential for targeted delivery. Secondly, the adhesion of nontargeted $Fe_3O_4@SiO_2$(FITC)-NH_2 and VCAM-1-targeted $Fe_3O_4@SiO_2$(FITC) nanoparticles was compared further under several sets of flow conditions. For both nontargeted $Fe_3O_4@SiO_2$(FITC)-NH_2 and VCAM-1-targeted $Fe_3O_4@SiO_2$(FITC) nanoparticles, their degree of adhesion decreased with increasing of shear stress (Figure 8) and duration of exposure to stress (Figure 9). Comparing Figures 8 and 9, the adhesion for each group was also found to show a shear-dependent relationship. The degree of nanoparticle adhesion decreased significantly when the exposed shear stresses increased from 1.1 to 9.94 dynes, indicating that interaction between the nanoparticles and HUVEC-CS depended on both shear stress and duration of exposure to stress. However, the degree of adhesion of VCAM-1-targeted $Fe_3O_4@SiO_2$(FITC) nanoparticles to endothelial cells was significantly greater than that of nontargeted $Fe_3O_4@SiO_2$(FITC)-

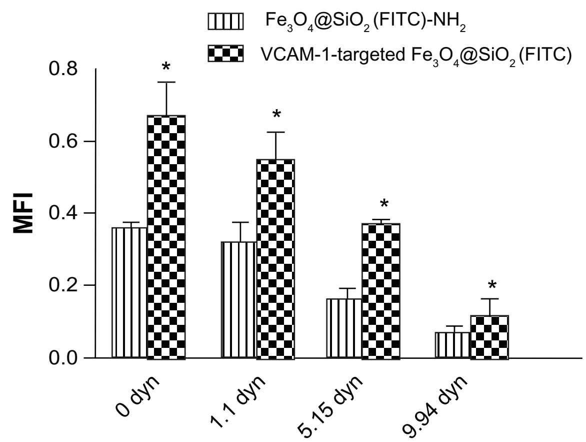

Figure 8 Adhesion of $Fe_3O_4@SiO_2$(FITC)-NH_2 and VCAM-1-targeted $Fe_3O_4@SiO_2$(FITC) nanoparticles under various exposures to shear stress for 3 minutes.

Notes: Fluorescent nanoparticles adhered on the monolayer of HUVEC-CS were quantified by calculating the MFI from six randomly selected microscopic fields (objective magnification 10×) for each group. *$P < 0.05$ versus $Fe_3O_4@SiO_2$(FITC)-NH_2 within each group.

Abbreviations: HUVEC-CS, an inflammatory subline of human umbilical vein endothelial cells; $Fe_3O_4@SiO_2$(FITC), fluorescein isothiocyanate-loaded silica-coated superparamagnetic iron oxide nanoparticles; VCAM-1, vascular cell adhesion molecule-1; MFI, mean fluorescence intensity.

NH_2 nanoparticles in the same experimental group. This specific adhesion could be used in clinical applications such as targeted magnetic resonance imaging or drug delivery to localized disease sites in the future.

To explore the biological applications of VCAM-1-targeted $Fe_3O_4@SiO_2$(FITC) nanoparticles further, their

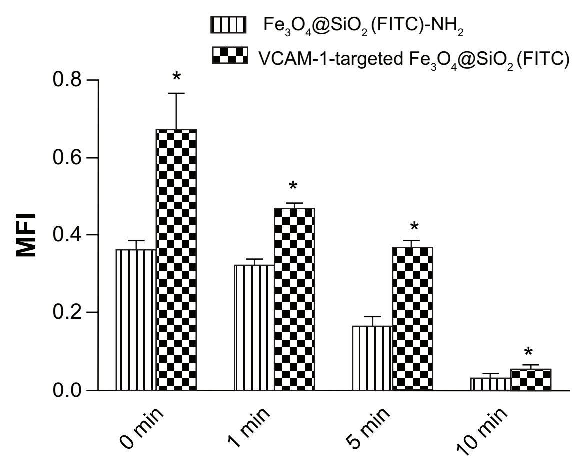

Figure 9 Time-dependent adhesion of $Fe_3O_4@SiO_2$(FITC)-NH_2 and VCAM-1-targeted $Fe_3O_4@SiO_2$(FITC) nanoparticles under exposure to shear stress of 5.15 dynes/cm^2.

Notes: The fluorescent nanoparticles adhered on the monolayer of HUVEC-CS were quantified by calculating the MFI for six random microscopic fields (objective magnification 10×) for each group. *$P < 0.05$ versus $Fe_3O_4@SiO_2$(FITC)-NH_2 within each group.

Abbreviations: HUVEC-CS, an inflammatory subline of human umbilical vein endothelial cells; $Fe_3O_4@SiO_2$(FITC), fluorescein isothiocyanate-loaded silica-coated superparamagnetic iron oxide nanoparticles; VCAM-1, vascular cell adhesion molecule-1; MFI, mean fluorescence intensity.

accumulation was investigated by confocal microscopy and flow cytometry under in vitro conditions. We first compared the cellular distribution and accumulation of nontargeted $Fe_3O_4@SiO_2$(FITC)-NH_2 and VCAM-1-targeted $Fe_3O_4@SiO_2$(FITC) nanoparticles without stimulation by lipopolysaccharide. It was found that there was no marked difference, as shown in Figure 10A. A low level of VCAM-1 expression was possible without applying lipopolysaccharide stimulation to HUVEC-CS.[15] However, the accumulation of VCAM-1-targeted $Fe_3O_4@SiO_2$(FITC) nanoparticles on the cell surfaces was considerably higher compared with nontargeted $Fe_3O_4@SiO_2$(FITC)-NH_2 nanoparticles (top two panels in Figure 10B). This was because of upregulation of VCAM-1 expression on lipopolysaccharide-activated endothelial cell surfaces causing more adhesion of VCAM-1-targeted $Fe_3O_4@SiO_2$(FITC) nanoparticles on HUVEC-CS. This phenomenon also existed in a magnetic field (third panel in Figure 10B). To verify whether adhesion is mediated via VCAM-1, lipopolysaccharide-activated HUVEC-CS were pretreated with anti-VCAM-1 monoclonal antibody to block the VCAM-1 receptors. Accumulation of VCAM-1-targeted $Fe_3O_4@SiO_2$(FITC) nanoparticles on the cell surfaces slightly decreased after pretreatment with the anti-VCAM-1 monoclonal antibody (the lowest panel in Figure 10B). It seems reasonable that some VCAM-1 receptors were occupied by anti-VCAM-1 monoclonal antibody, decreasing accumulation of VCAM-1-targeted $Fe_3O_4@SiO_2$(FITC) nanoparticles on HUVEC-CS. These data also suggest that VCAM-1-mediated adhesion is an important avenue for delivery of modified nanoparticles, and some other accumulation or cellular uptake mechanisms in addition to VCAM-1-mediated endocytosis may also be operating.[31,32] The quantitative accumulation of nanoparticles was further determined using detection of mean fluorescence intensity by flow cytometry, as shown in Figure 10C. The results agreed well with the data obtained by confocal microscopy. Our data showed that the VCAM-1-targeted $Fe_3O_4@SiO_2$(FITC) nanoparticles could be magnetically and biologically targeted to HUVEC-CS (ie, a dual-targeted delivery system).

To assess the magnetic sensitivity and imaging feasibility of VCAM-1-targeted $Fe_3O_4@SiO_2$(FITC) nanoparticles as biomedical probes, HUVEC-CS were treated with various concentrations of VCAM-1-targeted $Fe_3O_4@SiO_2$(FITC) nanoparticles. Magnetic measurement of the VCAM-1-targeted $Fe_3O_4@SiO_2$(FITC) nanoparticles at 300 K showed no hysteresis (Figure 6), indicating that they were superparamagnetic and favorable as T_2 magnetic resonance contrast agents. Figure 11A shows the image-darkening effect with increasing concentration of VCAM-1-targeted $Fe_3O_4@SiO_2$(FITC) nanoparticles. Because of their relatively low magnetization saturation, the contrast was more obvious at a high particle concentration of 400 µg/mL, indicating that the functionalized nanoparticles could be used as a probe in simultaneous T_2 magnetic resonance imaging and

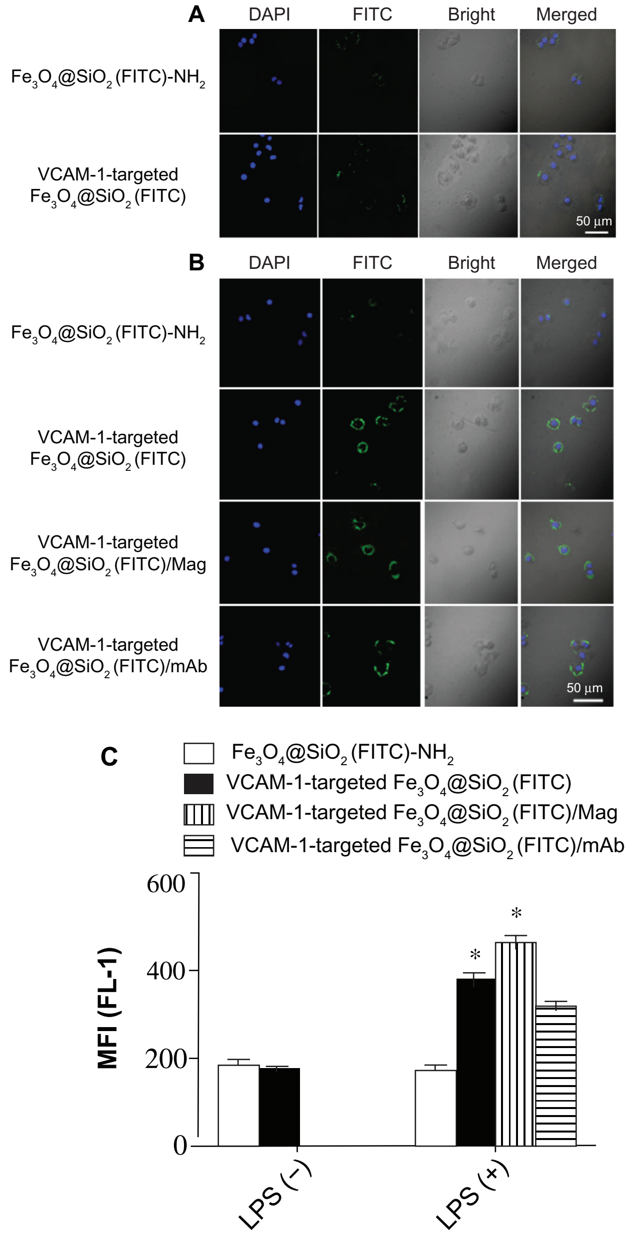

Figure 10 Confocal laser scanning microscopic images of HUVEC-CS after 4 hours of incubation with nanoparticles without (**A**) or with (**B**) LPS stimulation. Adherent particles with FITC labeling (green) and cell nuclei stained with DAPI (blue) were detected by confocal microscopy. (**C**) Quantitative assessment of nontargeted $Fe_3O_4@SiO_2$(FITC)-NH_2 and VCAM-1-targeted $Fe_3O_4@SiO_2$(FITC) nanoparticle accumulation in HUVEC-CS by flow cytometry.
Notes: MFI of FITC fluorescence in the cells was measured (n = 3, mean ± standard deviation). $^*P < 0.05$ versus $Fe_3O_4@SiO_2$(FITC)-NH_2 with LPS stimulation.
Abbreviations: HUVEC-CS, an inflammatory subline of human umbilical vein endothelial cells; $Fe_3O_4@SiO_2$(FITC), fluorescein isothiocyanate-loaded silica-coated superparamagnetic iron oxide nanoparticles; mAb, monoclonal antibody; VCAM-1, vascular cell adhesion molecule-1; MFI, mean fluorescence intensity.

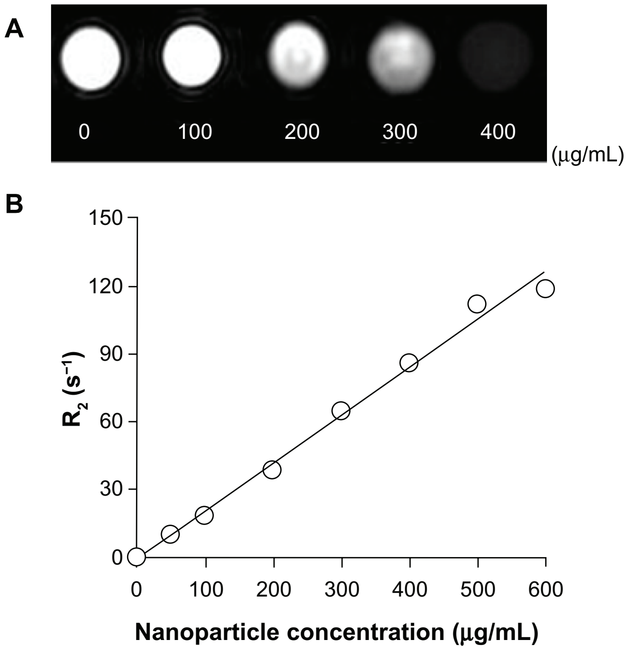

Figure 11 (**A**) T_2-weighted magnetic resonance images of HUVEC-CS treated with VCAM-1-targeted $Fe_3O_4@SiO_2$(FITC) nanoparticles at different concentrations, obtained using a 3.0 Tesla magnetic resonance scanner. (**B**) Relaxation (R_2) plot of VCAM-1-targeted $Fe_3O_4@SiO_2$(FITC) samples as a function of nanoparticle concentration shows that VCAM-1-targeted $Fe_3O_4@SiO_2$(FITC) retained good magnetism.

Abbreviations: HUVEC-CS, an inflammatory subline of human umbilical vein endothelial cells; $Fe_3O_4@SiO_2$(FITC), fluorescein isothiocyanate-loaded silica-coated superparamagnetic iron oxide nanoparticles; mAb, monoclonal antibody; VCAM-1, vascular cell adhesion molecule-1.

optical fluorescence imaging (FITC tracking). We also determined the T_2 relaxivity (R_2, efficiency of a contrast agent) of the VCAM-1-targeted $Fe_3O_4@SiO_2$(FITC) nanoparticles, and it was found that they retained good magnetism (Figure 11B).

Conclusion

We have developed a strategy for synthesis of novel multifunctional VCAM-1-targeted $Fe_3O_4@SiO_2$(FITC) nanoparticles with a diameter of 355 ± 37 nm, which are stable and well dispersed in aqueous solution. The interaction between VCAM-1-targeted $Fe_3O_4@SiO_2$(FITC) nanoparticles and HUVEC-CS under various flow conditions was evaluated further using a parallel plate flow chamber system. The VCAM-1-targeted $Fe_3O_4@SiO_2$(FITC) nanoparticles could adhere specifically to inflammatory endothelial cells activated by lipopolysaccharide, and their adherence depended on the shear stress and duration of exposure to stress. We also demonstrated that the VCAM-1-targeted $Fe_3O_4@SiO_2$(FITC) nanoparticles were able to accumulate specifically on cell surfaces and enter endothelial cells with high efficiency via VCAM-1-mediated binding. Moreover, we have demonstrated that VCAM-1-targeted $Fe_3O_4@SiO_2$(FITC) nanoparticles have potential as probes in magnetic resonance imaging. The possibility of selective delivery of VCAM-1-targeted $Fe_3O_4@SiO_2$(FITC) nanoparticles to sites of inflammation and their accumulation or uptake by targeted cells give them high potential in vascular magnetic resonance imaging for clinical diagnosis of cardiovascular disease, eg, atherosclerosis and thrombosis.

Disclosure

The authors report no conflicts of interest in this work.

Acknowledgments

Financial support for this work was provided in whole or in part by the National Natural Science Foundation of China (81071257, 81201192, 81101147, 11272083), the New Century Excellent Talents Program in Chinese Universities (NCET-09-0263), the Sichuan Youth Science and Technology Foundation of China (2010JQ0004), the Postdoctoral Program of China (2011M501297, 2012T50715), and the Fundamental Research Funds for Central Universities (ZYGX2010X019, ZYGX2010J101, ZYGX2011J099). The authors thank Jeng-Jiann Chiu from the National Health Research Institutes of Taiwan for his kind gift of the parallel flow chamber.

References

1. Zhang M, Cushing BL, O'Connor CJ. Synthesis and characterization of monodisperse ultra-thin silica-coated magnetic nanoparticles. *Nanotechnology*. 2008;19:085601.
2. Liu G, Wu H, Zheng H, et al. Synthesis and applications of fluorescent-magnetic-bifunctional-dansylated $Fe_3O_4@SiO_2$ nanoparticles. *J Mater Sci*. 2011;46:5959–5968.
3. Reddy LH, Arias JL, Nicolas J, Couvreur P. Magnetic nanoparticles: design and characterization, toxicity and biocompatibility, pharmaceutical and biomedical applications. *Chem Rev*. 2012;112:5818–5878.
4. Xia T, Kovochich M, Liong M, et al. Polyethyleneimine coating enhances the cellular uptake of mesoporous silica nanoparticles and allows safe delivery of siRNA and DNA constructs. *ACS Nano*. 2009;3: 3273–3286.
5. Lu Y, Yin Y, Mayers BT, Xia Y. Modifying the surface properties of superparamagnetic iron oxide nanoparticles through a sol-gel approach. *Nano Lett*. 2002;2:183–186.
6. Graf C, Vossen DLJ, Imhof A, van Blaaderen A. A general method to coat colloidal particles with silica. *Langmuir*. 2003;19:6693–6700.
7. Lu CW, Hung Y, Hsiao JK, et al. Bifunctional magnetic silica nanoparticles for highly efficient human stem cell labeling. *Nano Lett*. 2007;7: 149–154.
8. Yang J, Lee J, Kang J, et al. Magnetic sensitivity enhanced novel fluorescent magnetic silica nanoparticles for biomedical applications. *Nanotechnology*. 2008;19:075610.
9. Jing L, Yang C, Qiao R, et al. Highly fluorescent CdTe@SiO_2 particles prepared via reverse microemulsion method. *Chem Mater*. 2010;22:420–427.
10. Zhang G, Feng J, Lu L, Zhang B, Cao L. Fluorescent magnetic nanoprobes: design and application for cell imaging. *J Colloid Interface Sci*. 2010;351:128–133.
11. He R, You X, Shao J, Gao F, Pan B, Cui D. Core/shell fluorescent magnetic silica-coated composite nanoparticles for bioconjugation. *Nanotechnology*. 2007;18:18315601.

12. Conversano F, Greco A, Casciaro E, Ragusa A, Lay-Ekuakille A. Harmonic ultrasound imaging of nanosized contrast agents for multimodal molecular diagnoses. *IEEE Trans Instrum Meas*. 2012; 61(7):1848–1856.
13. Malvindi MA, Greco A, Conversano F, et al. Magnetic/silica nanocomposites as dual-mode contrast agents for combined magnetic resonance imaging and ultrasonography. *Adv Funct Mater*. 2011;21:2548–2555.
14. Casciaro S, Conversano F, Ragusa A, et al. Optimal enhancement configuration of silica nanoparticles for ultrasound imaging and automatic detection at conventional diagnostic frequencies. *Invest Radiol*. 2010;45:715–724.
15. Yang H, Xiong X, Zhang L, Wu C, Liu Y. Adhesion of bio-functionalized ultrasound microbubbles to endothelial cells by targeting to vascular cell adhesion molecule-1 under shear flow. *Int J Nanomedicine*. 2011;6:2043–2051.
16. McAteer MA, Schneider JE, Ali ZA, et al. Magnetic resonance imaging of endothelial adhesion molecules in mouse atherosclerosis using dual-targeted microparticles of iron oxide. *Arterioscler Thromb Vasc Biol*. 2008;28:77–83.
17. Wan J, Meng X, Liu E, Chen K. Incorporation of magnetite nanoparticle clusters in fluorescent silica nanoparticles for high-performance brain tumor delineation. *Nanotechnology*. 2010;21:235104.
18. Liu Y, Shi M, Xu M, Yang H, Wu C. Multifunctional nanoparticles of Fe_3O_4@SiO_2(FITC)/PAH conjugated the recombinant plasmid of pIRSE2-EGFP/$VEGF_{165}$ with dual functions for gene delivery and cellular imaging. *Exp Opin Drug Deliv*. 2012;9:1197–1207.
19. Meng G, Liu Y, Lou C, Yang H. Emodin suppresses lipopolysaccharide-induced pro-inflammatory responses and NF-kappaB activation by disrupting lipid rafts in CD14-negative endothelial cells. *Br J Pharmacol*. 2010;161:1628–1644.
20. Liu Y, Zhao F, Gu W, Yang H, Meng Q, Zhang Y, et al. The roles of platelet GPIIb/IIIa and αvβ3 integrins during HeLa cells adhesion, migration, and invasion to monolayer endothelium under static and dynamic shear flow. *J Biomed Biotechnol*. 2009;2009:829243.
21. Lee DY, Li YS, Chang SF, et al. Oscillatory flow-induced proliferation of osteoblast-like cells is mediated by αvβ3 and beta1 integrins through synergistic interactions of focal adhesion kinase and shc with phosphatidylinositol 3-kinase and the AKT/mTOR/p70 s6k pathway. *J Biol Chem*. 2010;285:30–42.
22. Deng Y-H, Wang C-C, Hu J-H, Yang W-L, Fu S-K. Investigation of formation of silica-coated magnetite nanoparticles via sol-gel approach. *Colloids Surf A Physicochem Eng Asp*. 2005;262:87–93.
23. Liu Y, Lou C, Yang H, Shi M, Miyoshi H. Silica nanoparticles as promising drug/gene delivery carriers and fluorescent nano-probes: recent advances. *Curr Cancer Drug Targets*. 2011;11:156–163.
24. Shi M, Liu Y, Xu M, Yang H, Wu C, Miyoshi H. Core/shell Fe_3O_4@SiO_2 nanoparticles modified with PAH as a vector for EGFP plasmid DNA delivery into HeLa cells. *Macromol Biosci*. 2011;11:1563–1569.
25. LaConte LE, Nitin N, Zurkiya O, et al. Coating thickness of magnetic iron oxide nanoparticles affects R_2 relaxivity. *J Magn Reson Imaging*. 2007;26:1634–1641.
26. Samuel SP, Jain N, O'Dowd F, et al. Multifactorial determinants that govern nanoparticle uptake by human endothelial cells under flow. *Int J Nanomedicine*. 2012;7:2943–2956.
27. Wang Z, Guo Y, Li S, Sun Y, He N. Synthesis and characterization of SiO_2/(PMMA/Fe_3O_4) magnetic nanocomposites. *J Nanosci Nanotechnol*. 2008;8:1797–1802.
28. Lawrier GA, Battersby BJ, Trau M. Synthesis of optically complex core-shell colloidal suspensions: pathways to multiplexed biological screening. *Adv Funct Mater*. 2003;13:887–896.
29. Lee JE, Lee N, Kim H, et al. Uniform mesoporous dye-doped silica nanoparticles decorated with multiple magnetite nanocrystals for simultaneous enhanced magnetic resonance imaging, fluorescence imaging, and drug delivery. *J Am Chem Soc*. 2010;132:552–557.
30. Loken MR, Lanier LL. Three-color immunofluorescence analysis of leu antigens on human peripheral blood using two lasers on a fluorescence-associated cell sorter. *Cytometry*. 1984;5:151–158.
31. Yang H, Lou C, Xu M, Wu C, Miyoshi H, Liu Y. Investigation of folate-conjugated fluorescent silica nanoparticles for targeting delivery to folate receptor-positive tumors and their internalization mechanism. *Int J Nanomedicine*. 2011;6:2023–2032.
32. Xu Z, Chen L, Gu W, et al. The performance of docetaxel-loaded solid lipid nanoparticles targeted to hepatocellular carcinoma. *Biomaterials*. 2009;30:226–232.